Supporting Information for:

Crystallization-Induced Room-Temperature Phosphorescence in Fumaramides

Andrea Nitti, Chiara Botta, Alessandra Forni,* Elena Cariati, Elena Lucenti, Dario Pasini**

Table of Contents

1. General Experimental

Synthesis. All commercially available reagents and solvents were purchased from Sigma-Aldrich, Fluorochem and Alfa Aesar. They were all used as received. Flash chromatography was carried out using Merck silica gel 60 (pore size 60 Å, 270-400 Mesh). ^{1}H and ^{13}C NMR spectra were recorded from solutions in deuterated solvents on 200, 300 and 400 MHz spectrometers using the residual solvent peak as the reference. Low resolution mass spectra of pure compounds were recorded using Agilent Technologies ESI-MS Spectrometer instrument. Samples for the ESI-MS experiment were dissolved in a mixture of THF/MeOH 1:1.

Spectroscopy. UV-Visible spectra were collected by Perkin-Elmer Lambda900 spectrophotometer. The solid UV-Vis diffuse reflectance spectra were recorded using a Shimadzu UV3600 spectrophotometer with $BaSO_4$ as a reference. Steady state emission and excitation spectra and photoluminescence lifetimes were obtained using both a FLS 980 (Edinburg Instrument Ltd) and a Nanolog (Horiba Scientific) spectrofluorimeter composed of iH320 spectrograph equipped with a Synapse QExtra charge-coupled device. The spectra are corrected for the instrument response. Phosphorescence spectra are obtained with a PPD-850 single photon detector module with time-gated separation by exciting with a pulsed Xe lamp. Time-resolved TCSPC measurements are obtained with PPD-850 single photon detector module and DeltaTime serie DD-300 DeltaDiode and DD-405L DeltaDiode Laser and analysed with the instrument Software DAS6.

X-Ray Crystallography. Crystal samples of compounds **1** and **2** were mounted on glass fibres in air and collected at 293 and 120 K, respectively, on a Bruker AXS APEX2 CCD area-detector diffractometer. Graphite-monochromatized Mo-Kα (λ = 0.71073 Å) radiation was used with the generator working at 50 kV and 35 mA. The intensity data were collected in the full sphere; an empirical absorption correction was applied (SADABS). The structure was solved by direct methods (ShelxS)[S2] and refined with full-matrix least squares (SHELX-2014)[S2] on F^2; anisotropic temperature factors were assigned to all non-hydrogen atoms. Hydrogens were riding on their carbon atoms. CCDC reference numbers: 2020250 (**1**), 2020251 (**2**). XRD of powders were acquired from 7° to 40° through 0.02° increments.

Theoretical calculations. The molecular structures of compounds **1-3** have been optimized in vacuo within the DFT approach, using the ωB97X functional[S3] which has previously been judged well suited for describing

the electronic features of a series of organic dyes.[S4] The X-ray diffraction structures of **1** and **2** have been used as starting point for geometry optimization, while for compound **3** the molecular structure derived from resolution of a geminated crystal of **3** has been used. The 6-311++G** basis set was chosen for all atoms. Using the ωB97X/6-311++G** optimized geometries, standard vertical Time Dependent DFT (TDDFT) calculations have been carried out at the same level of theory to determine the singlet and triplet excitation energy levels.

2. Synthetic Procedures

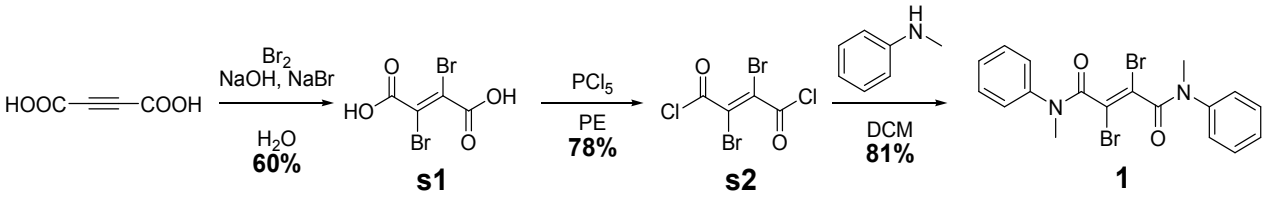

Scheme S1. Synthesis of compound **1**

Compounds **s1** and **s2** were synthesized according to literature.[S5]

2,3-dibromofumaric acid (s1). A solution of Br_2 (761 μL, 10 mmol, 1 eq) in water (5 mL) was added dropwise at 0°C to a solution of but-2-ynedioic acid (1,14 g, 10 mmol, 1 eq), NaOH (800 mg, 20 mmol, 2 eq.), NaBr (10, 29 g, 100 mmol, 10 eq.) in water (10 mL). The reaction mixture was kept for 2 h at 0°C and then a 1M HCl solution was added. The precipitate was filtrated and washed with water. Compound **s1** was obtained as beige solid (1,64 g, 60%).

2,3-dibromofumaroyl dichloride (s2). PCl_5 (3.8 g, 18.26 mmol, 5 eq.) was added to a suspension of compound **s3** (1 g, 3.65 mmol, 1 eq) in dry petroleum ether at 0°C. The reaction mixture was allowed to warm to room temperature and stirred for additional 12 h. The reaction mixture was filtrated to remove impurities and side products, and the solvent removed *in vacuo*. The solid crude product obtained was used in the next step without further purification.

2,3-Dibromo-*N*,*N*-dimethyl-*N*,*N*-diphenylfumaramide (1). Compound **s1** (745 mg, 2 mmol, 1 eq) was added under nitrogen to a solution of *N*-methylaniline (432 μL, 4 mmol, 2 eq) and potassium carbonate (552 mg, 4 mmol, 2 eq) in DMF (10 mL). The solution was stirred overnight and the solvent was removed *in vacuo*. The crude reaction mixture was purified by flash chromatography using *n*-hexane and ethyl acetate (9:1, v/v) as the eluent. Compound **1** was obtained as a white solid (812 mg, 81%). R_f = 0.77. ^{1}H NMR (300 MHz, $CDCl_3$) δ: 7.20–7.60 (m, 10H, **ArH**-), 3.4-2.6 (series of singlets, 6H, C**H**$_3$N-). ^{13}C NMR (75 MHz, $CDCl_3$) δ: 162.5, 141.1 , 129.4, 129.2, 129.0, 128.6, 128.35, 127.1, 126.8, 126.1, 125.2, 37.3, 37.1. GC-MS(EI) *rt:* 20.49 min; *m/z:* 452 $[M]^+$.

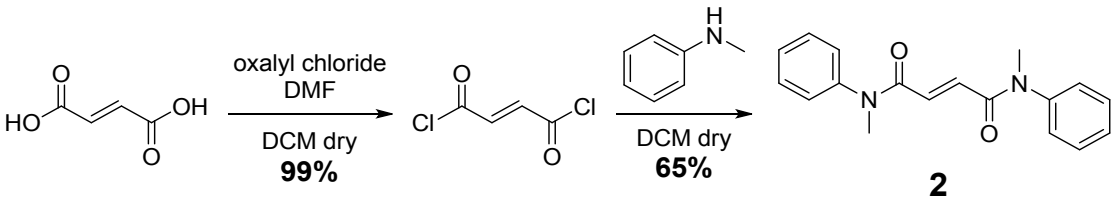

Scheme S2. Synthesis of compound **2**

***N*, *N*-dimethyl-*N*, *N*-diphenylfumaramide (2).** Oxalyl chloride (552 mg, 4 mmol, 2 eq) and 5 drops of DMF were added dropwise to a suspension of fumaric acid (1.16 g, 10 mmol, 1 eq) in dry DCM at 0°C. The reaction mixture was allowed to room temperature and stirred for 12 h. The solvent was then removed *in vacuo* and the crude reaction mixture containing fumaroyl dichloride was dissolved in dry DCM (5 mL) and added dropwise to a solution of *N*-methylaniline (864 μL, 8 mmol, 4 eq) in dry DCM (10 mL) under nitrogen and stirred overnight. The solvent was removed under reduced pressure. The crude product was purified by flash chromatography using n-hexane and ethyl acetate (9:1, v/v) as eluent. Compound **2** was obtained as white solid (1.8 g, 65%). ^{1}H NMR (300 MHz, $CDCl_3$) δ: 7.49–7.31 (m, 6H, **ArH**-), 7.14 (d, J = 7.9 Hz, 4H, **ArH**-), 6.87 (s, 2H, -C**H**=C**H**-), 3.32 (s, 6H, C**H**$_3$N-). ^{13}C NMR (75 MHz, $CDCl_3$) δ: 162.1 (**C**O), 148.5 (**Ar**), 136.4 (-**C**H=**C**H-), 129.3 (**Ar**), 122.7 (**Ar**), 112.5 (**Ar**), 39.0 (**C**H$_3$-). ESI-MS *m/z:* 295 $[M + 1]^+$, 589 $[2M + 1]^+$.

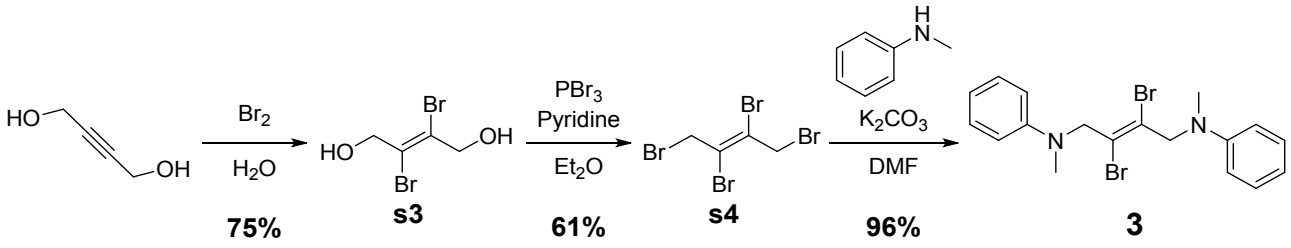

Scheme S3. Synthesis of compound **3**

Compounds **s3** and **s4** were synthesized according to literature procedures.[S6]

(*E*)-2,3-Dibromobut-2-ene-1,4-diol (s3). But-2-yne-1,4-diol (2.30 g, 26.54 mmol) was dissolved in water (50 mL) and cooled to 0°C. Bromine (1.8 mL, 35.0 mmol) was added dropwise. The resultant light-yellow solution was stirred at 0°C for 30 min and for an additional 90 min at room temperature. The reaction was quenched with a small amount of saturated $Na_2S_2O_3$ solution and neutralized by addition of 1 M NaOH. After extraction

with AcOEt the combined organic layers were dried over Na_2SO_4, filtered through silica gel and the solvent was removed *in vacuo* to afford the title compound as a white solid (5.94 g, 91%). ^{1}H NMR (200 MHz, DMSO-d_6) δ: 5.48 (t, J = 6.0 Hz, 2H), 4.28 (d, J = 6.0 Hz, 4H).

(*E*)-1,2,3,4-tetrabromobut-2-ene (s4). Phosphorus tribromide (0.6 mL, 6.50 mmol) was slowly added to a solution of **s1** (2 g, 8.13 mmol) and pyridine (0.1 mL, 1.46 mmol) in dry Et_2O (10 mL) at 0°C. The solution was stirred at 0°C for 30 min then heated at reflux for 4 h. After cooling, the reaction was quenched with water and the aqueous layer was extracted with Et_2O. The combined organic extracts were washed with a saturated $NaHCO_3$ aqueous solution, brine and dried over Na_2SO_4. The solution was passed through a silica gel plug and the solvent removed *in vacuo* to afford the title compound as a white solid (2.07 g, 70%).

(*E*)-2,3-dibromo-N_1, N_4-dimethyl-N_1, N_4-diphenylbut-2-ene-1,4-diamine (3). Compound **s4** (745 mg, 2 mmol, 1 eq) was added to a solution of *N*-methylaniline (432 μL, 4 mmol, 2 eq) and potassium carbonate (552 mg, 4 mmol, 2 eq) in DMF (10 mL) under nitrogen. After TLC monitoring, in which is observed a new spot (R_f = 0.77, H/A 9:1), solvent was removed under reduced pressure, than 20 mL of water was added and precipitate collected by filtration and dried in vacuum. Compound **3** was obtained as a white solid (812 mg, 95%). ^{1}H NMR (200 MHz, $CDCl_3$) δ: 7.35 (t, J = 7.33, 2H, **Ar**-), 6.82 (t, J = 7.33, 3H, **Ar**-), 4.58 (s, 4H, -C**H**$_2$-), 3.12 (s, 6H, C**H**$_3$-N-). ^{13}C NMR (75 MHz, $CDCl_3$) δ: 148.5 (**Ar**), 129.1 (**Ar**), 122.8 (**Ar**), 117.2 (-**C**Br=**C**Br-), 112.5 (**Ar**), 59.5 ,(-**C**H$_2$-), 39.0 (**C**H$_3$-). ESI-MS *m/z:* 425 $[M + 1]^+$.

3. Additional NMR Experiments

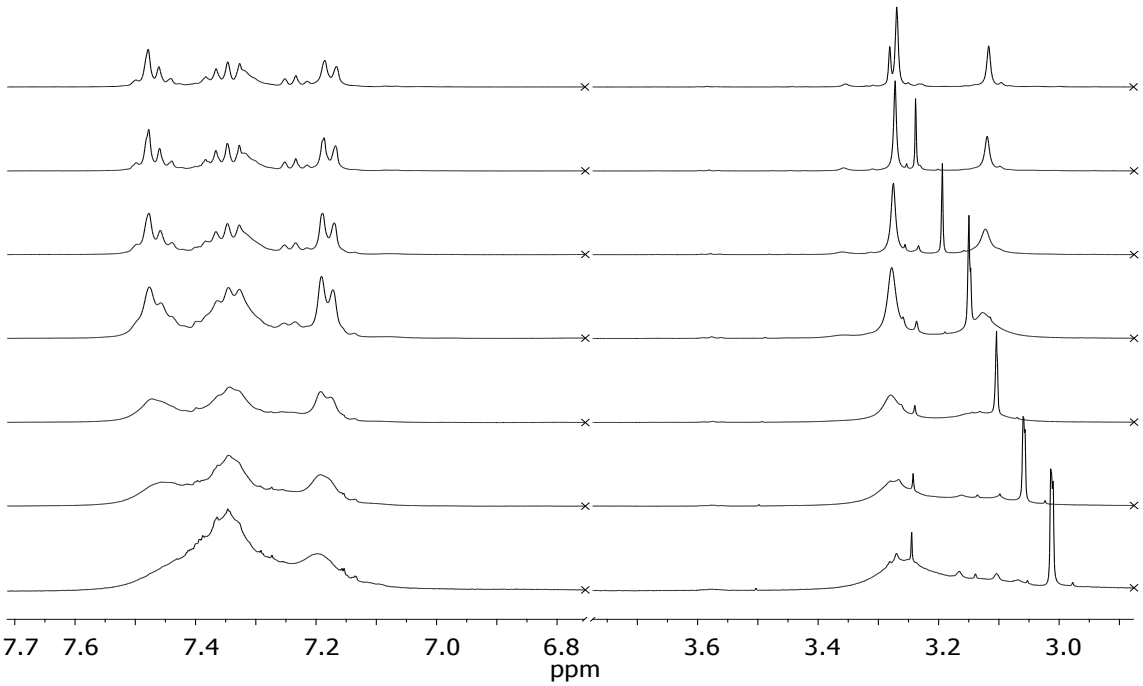

Figure S1. Temperature-dependent ^{1}HNMR spectra (400 MHz) of compound **1** in DMSO-d_6. From top to bottom: 25 °C, 35 °C, 45 °C, 55 °C, 65 °C, 75 °C, 85 °C.

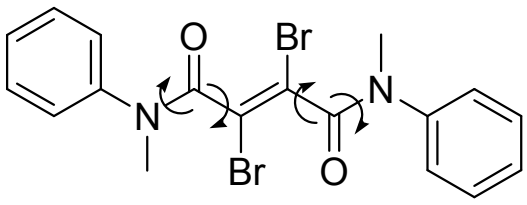

Compound **1**

The room temperature ^{1}H NMR spectra of compound **1** in DMSO-d_6 (400 MHz, Figure S1) and $CDCl_3$ (300 MHz, SI below) show the presence of different conformers, for example a series of singlets between 3.5 and 2.5 ppm, corresponding to the resonances of the methyl groups. The conformations are unequally populated, and their interconversion is slow on the NMR timescale up to 400 MHz. The presence of a conformational

equilibria is directly confirmed by the coalescence of the signals that occur at higher temperatures (Figure S1). The visualization of several conformers in the NMR spectra is the consequence of significant energetic barriers to the free rotation around: a) the carbonyl carbon-nitrogen bond (C–N) due to the conjugation of the nitrogen lone pair with the carbonyl moiety (C=O); b) the carbonyl carbon-double bond carbon (C-C), since the carbonyl can also conjugate on the other side with the carbon-carbon double bond. Rotations related to a) are commonly found in amides. For example, DMF shows two signals for its methyl resonances in the ^{1}H NMR spectrum at room temperature.

In compound **2**, however, all conformational equilibria are already fast on the NMR timescale at room temperature. Unlike simple amides, in **2** the availability of the carbonyl to conjugate with the amide nitrogen is reduced since in this case the carbonyl can also conjugate on the other side with the double bond. The sterically hindering bromine atoms contribute significantly to raise the energy barriers in the case of **1**.

4. Additional Computational Experiments

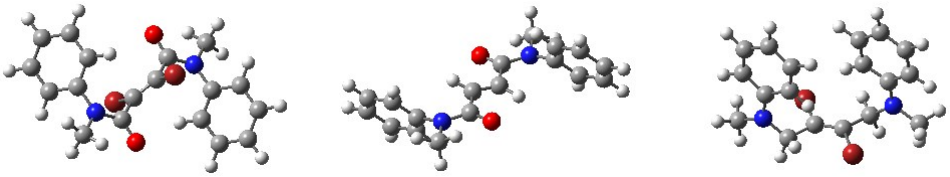

Figure S2. ωB97X/6-311++G(d,p) optimized structures of compounds **1** (left), **2** (center) and **3** (right).

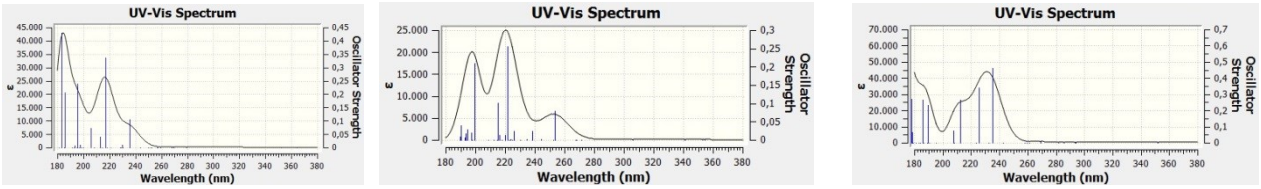

Figure S3. TDωB97X/6-311++G(d,p) computed absorption spectrum of compounds **1** (left), **2** (center) and **3** (right), resulting from convolution of the excitation energies (blue sticks) with 0.20 eV of half-bandwidth.

5. Additional Spectroscopic Experiments

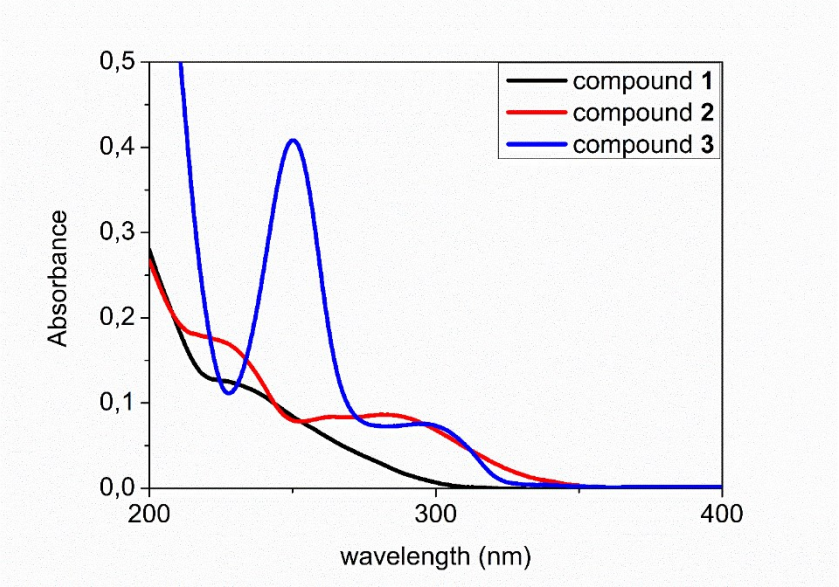

Figure S4. Absorption spectra of compound **1, 2** and **3** in solution (ACN, 10^{-5} mol·L^{-1}).

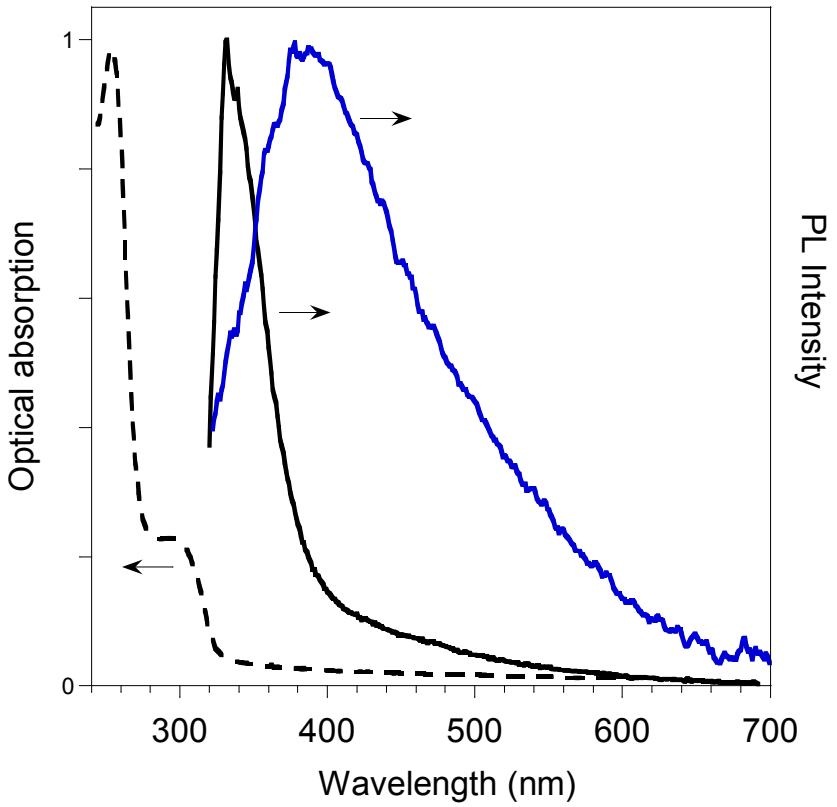

Figure S5. Absorption spectrum of compound **3** (black dashed line) and PL spectra (λ_{ex} = 300 nm) at room temperature (black solid line) and 77 K (blue solid line) in ACN (2 x 10^{-5} M).

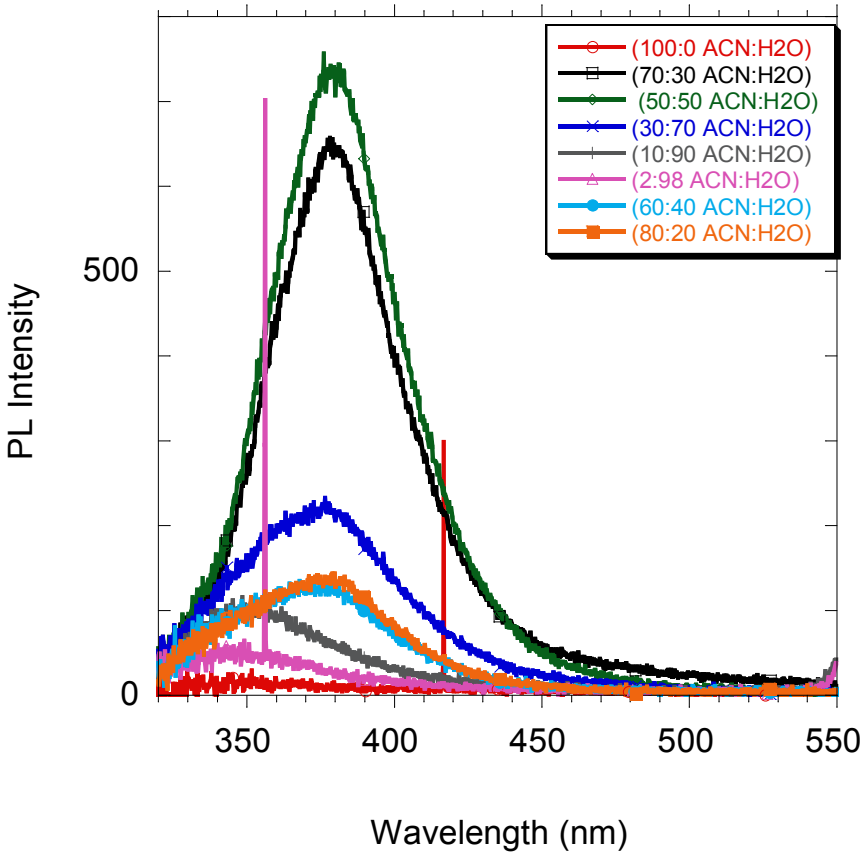

Figure S6. PL spectra of compound **3** in ACN/water solvent mixtures at different f_w values (solution 10^{-5} M, λ_{ex} = 280 nm)

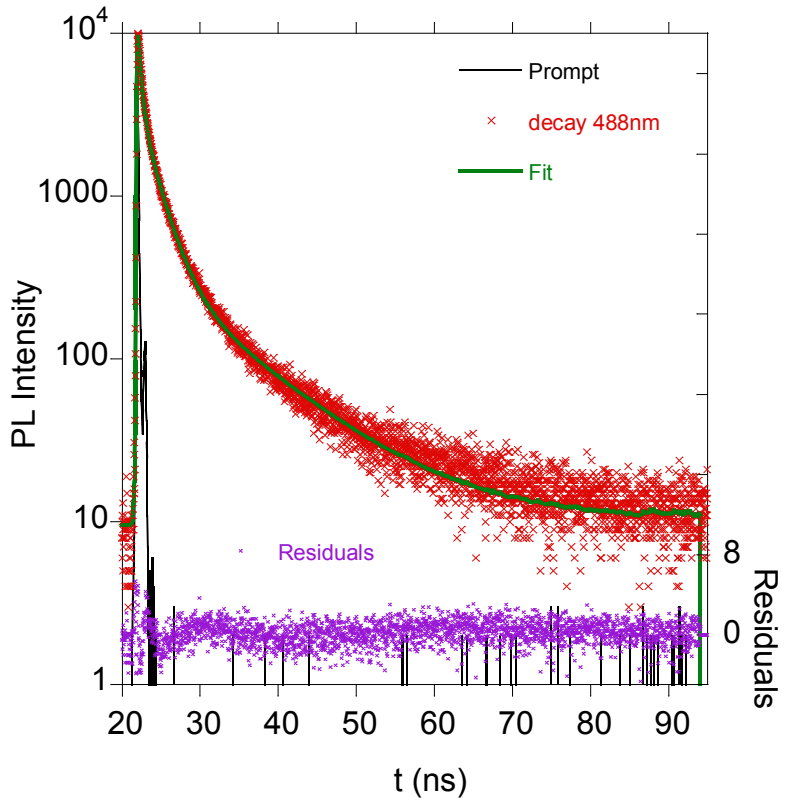

a1	τ_1	a2	τ_2	a3	τ_3	χ^2	$<\tau>$	τ_{av}
0,04375	2,127931	0,00454	10,76129	0,145177	0,36314	1,455324	1,006225	3,816638

Figure S7. PL decay of compound **1** as crystalline powder (red, λ_{ex} = 410 nm, emission 488 nm), and three-exponential fitting (green line, results are shown in the table).

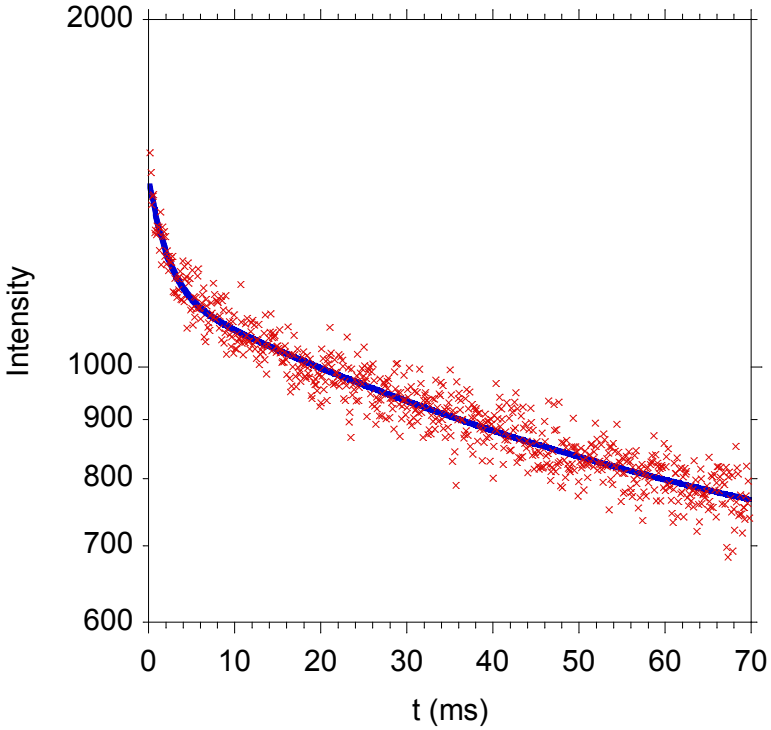

a1		τ_1		a2		τ_2		Statistics		<τ>	τ_{av}
Value	Std Error	Value	Std Error	Value	Std Error	Value	Std Error	χ^2	R^2	Value	Value
555,7668	1,58E+07	56,4381	6,39923	235,828	1,81E+08	2,09434	0,23675	1227,816	0,9347	40,24828	55,59565

Figure S8. Ph decay of compound **1** as crystalline powder (red, λ_{ex} = 410 nm, emission 580 nm), and two-exponential fitting (blue line, results are shown in the table).

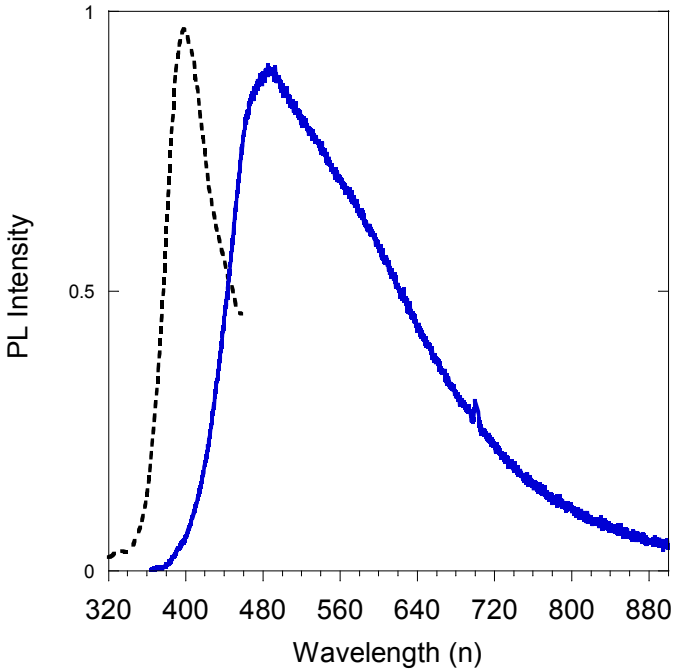

Figure S9. PL (blue line, excitation 350 nm) and PLE (black dashed line, emission 490 nm) spectra of crystalline powders of compound **2**.

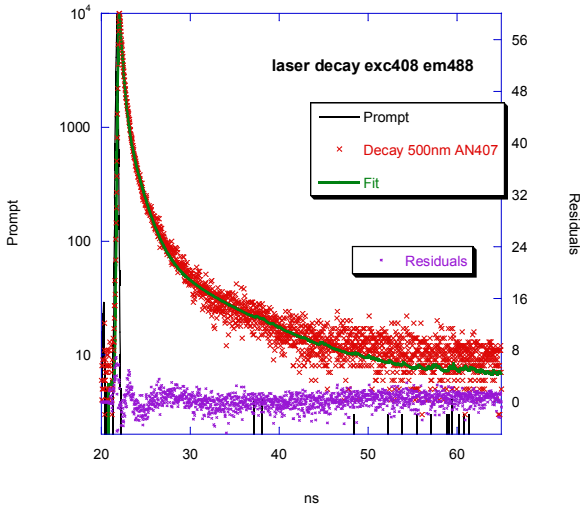

a1	τ_1	a2	τ_2	a3	τ_3	χ^2	<τ>	τ_{av}
0,026759	1,286283	0,001383	8,615031	0,204696	0,302626	1,543648	0,46506	1,530169

Figure S10. PL decay of compound **3** as crystalline powder (red x, λ_{ex} = 407 nm, emission at 500 nm) and three-exponential fitting (green line, results are shown in the table).

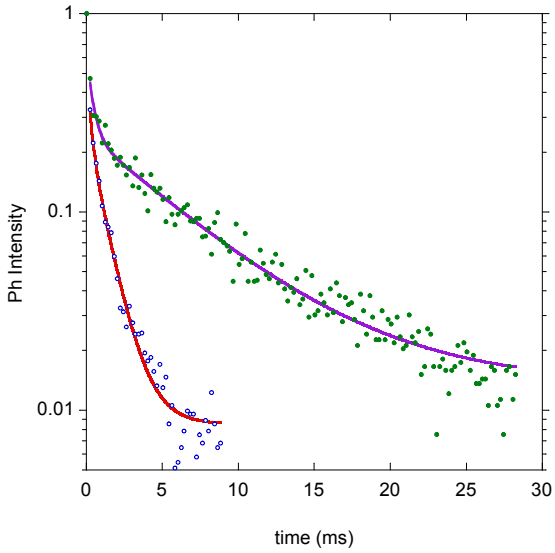

a1		τ_1		a2		τ_2		Statistics		<τ>	τ_{av}
Value	Std Error	Value	Std Error	Value	Std Error	Value	Sd Error	χ^2	R^2	Value	Value
0,28815	470054,2	0,39468	0,04986	0,22899	23196,9	6,35583	0,37129	1,38E-04	0,97322	3,034282	5,923784

a1		τ_1		a2		τ_2		Statistics		<τ>	τ_{av}
Value	Std Error	Value	Std Error	Value	Std Error	Value	Std Error	χ^2	R^2	Value	Value
0,21045	63672,63	1,12107	0,07815	0,1198	184036,2	0,22079	0,04523	1,92E-05	0,99544	0,794488	1,030312

Figure S11. Ph decay of compound **3** as crystalline powder: Excitation 390nm, emission 570 nm (open blue circles) and 676 nm (solid green circles), and two-exponential fitting (violet and red line, the results are shown in the tables).

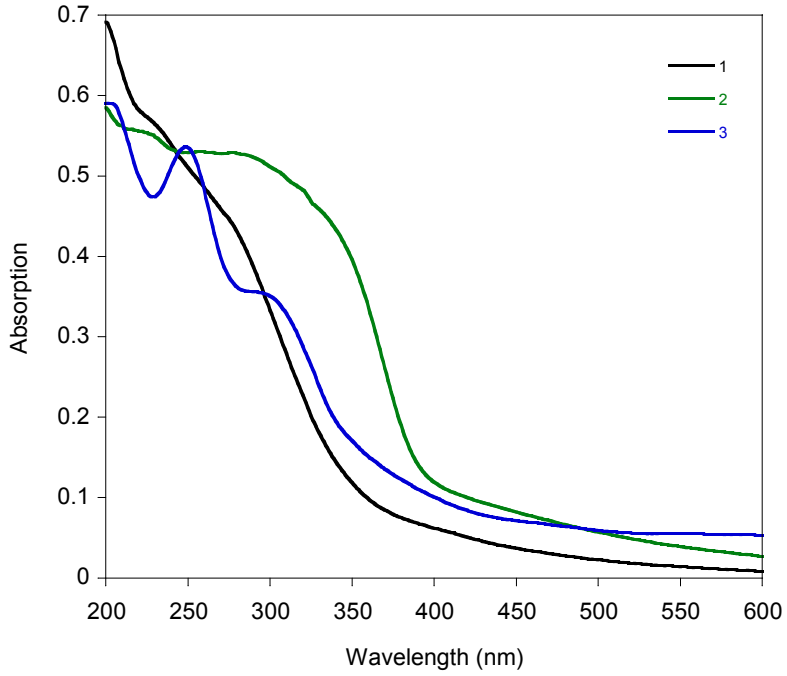

Figure S12. Absorption spectra of crystalline powders of compound **1, 2** and **3** obtained from diffuse reflectance spectra.

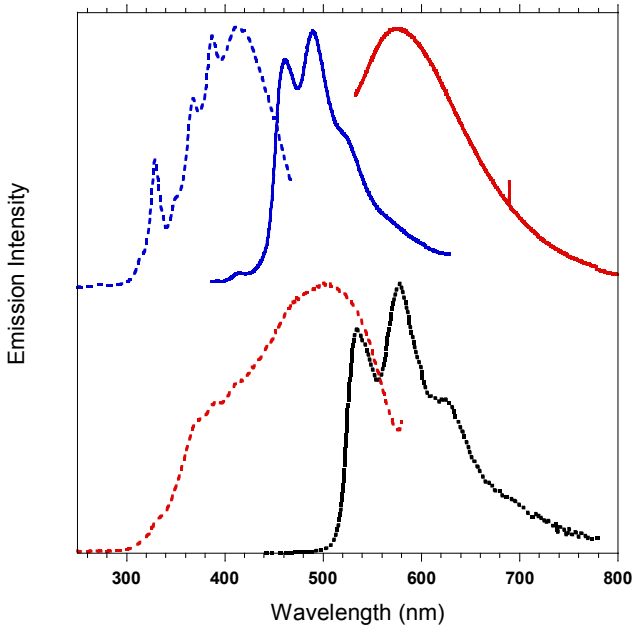

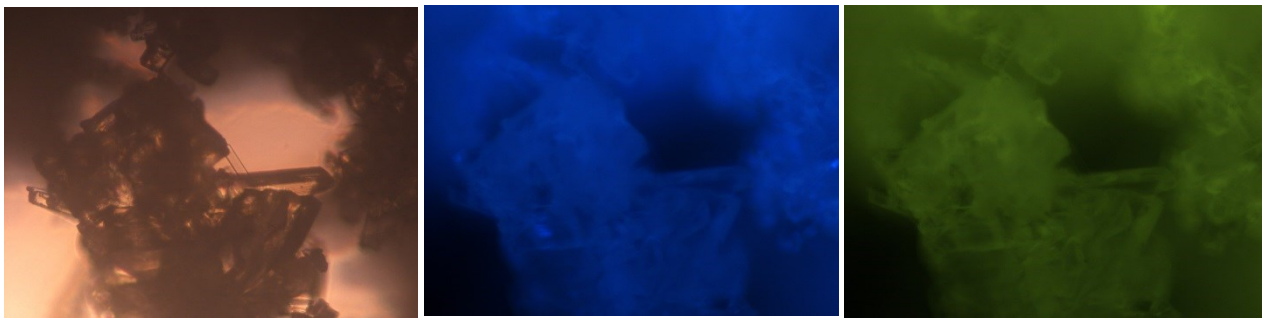

Figure S13. Top: PL, PLE and phosphorescence spectra of compound **1** as crystalline powders. Top: PL (exc 330nm, blue line, exc 500nm red line) and PLE (em490nm, blue dashed line). Bottom: PLE (em 600nm, red dashed line) and Phopshorescence (exc410nm delay 1ms, window 10ms). Bottom: Microscopy images of crystalline powders of compound **1** (optical microscopy, left; fluorescence microscopy, UV excitation, middle; blue excitation, right).

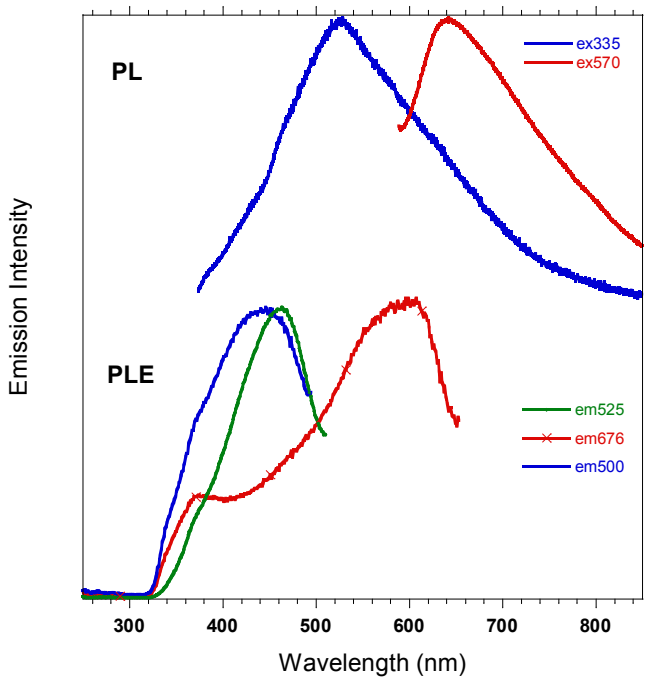

Figure S14.PL and PLE spectra of compound **3** as crystalline powders.

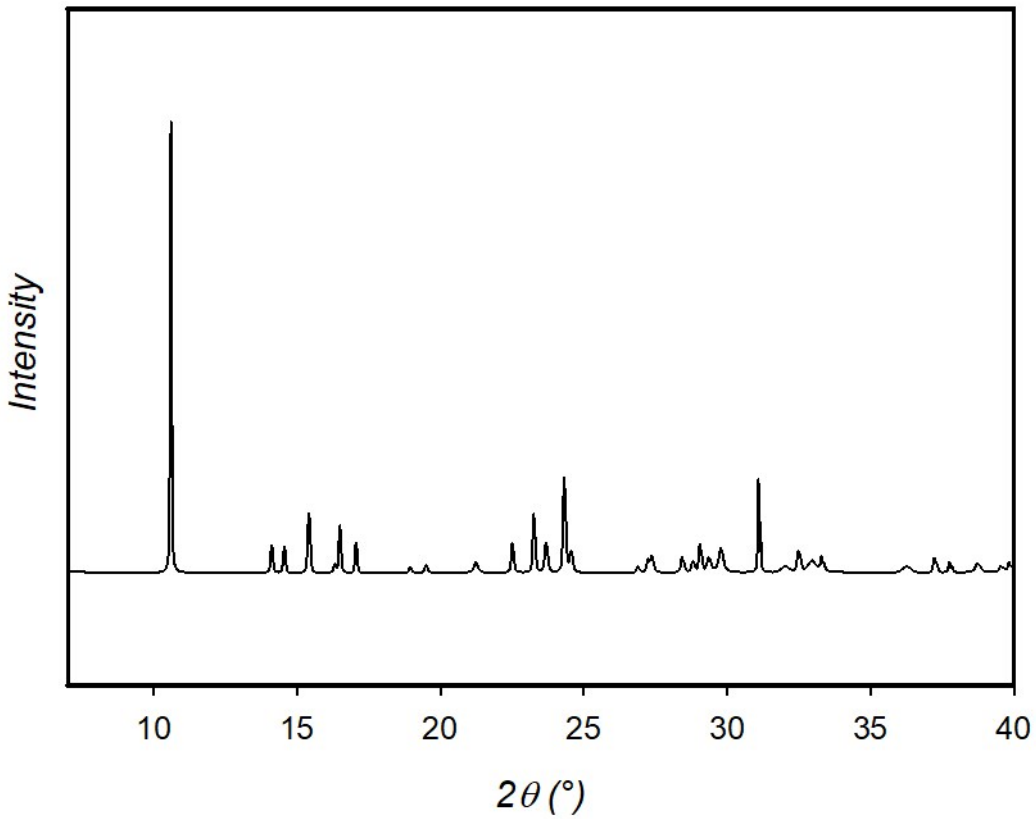

Figure S15. PXRD patterns of compound **1**

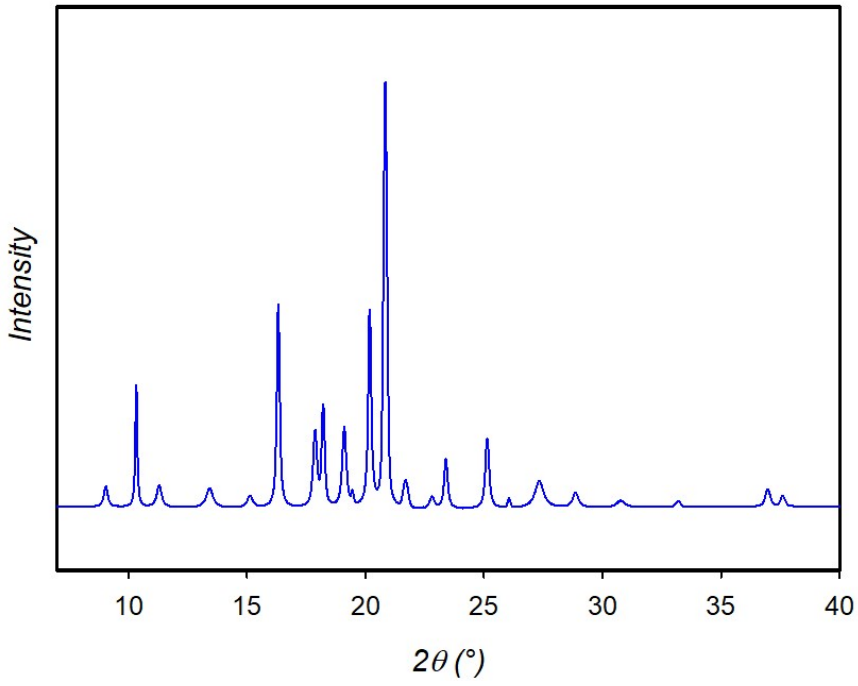

Figure S16. PXRD patterns for compound **2**

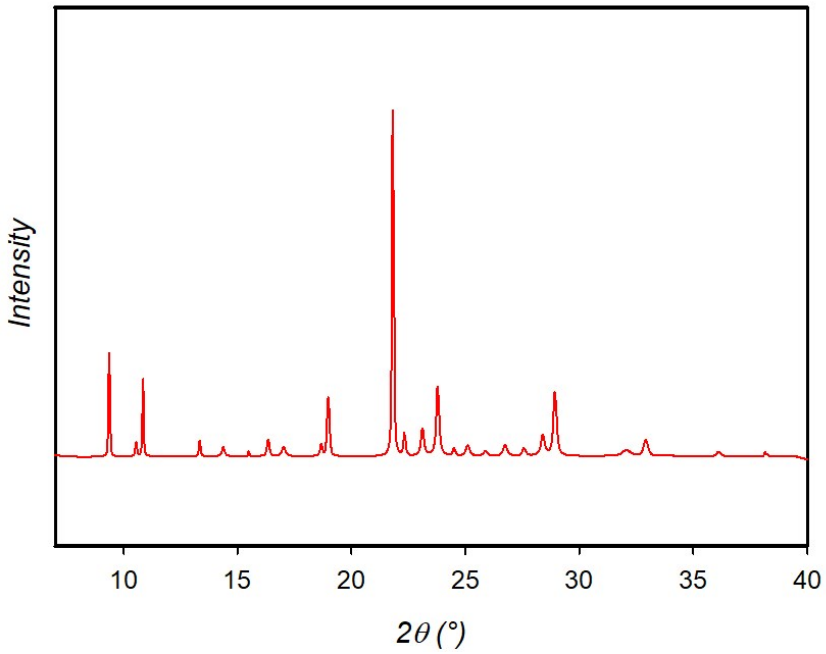

Figure S17. PXRD patterns for compound **3**

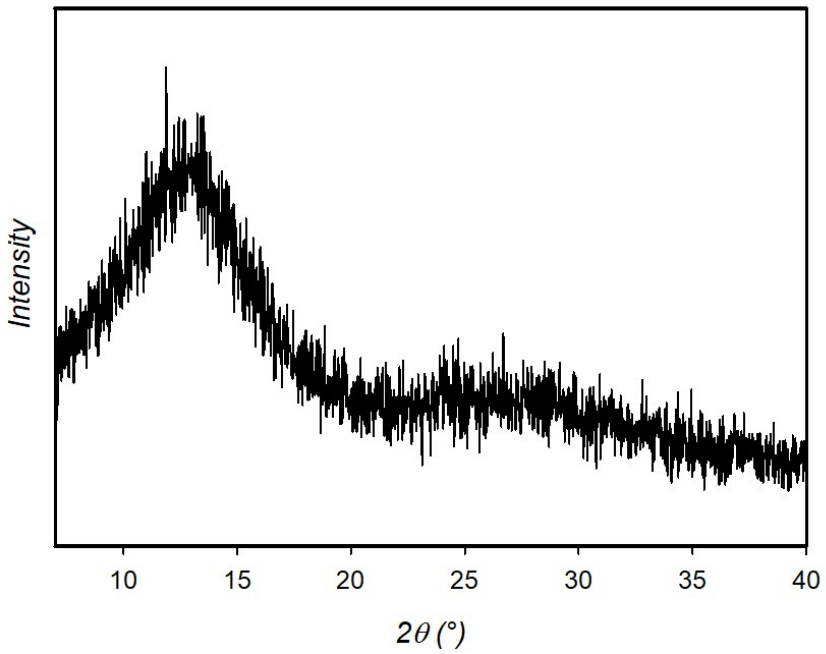

Figure S18. PXRD patterns for compound **1** in the amorphous state, obtained by melting and quickly cooling the crystalline powders.

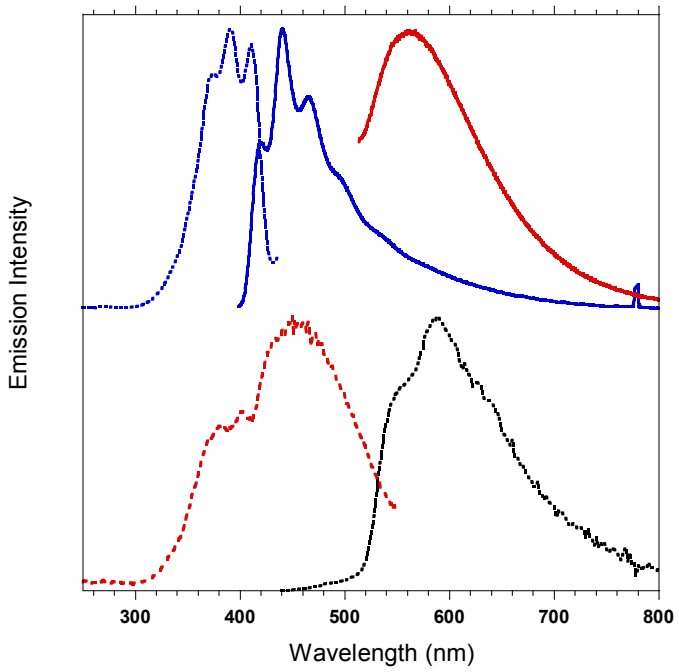

Figure S19. Top: PL, PLE and phosphorescence spectra of compound **1** as amorphous. Top: PL (λ_{ex}= 390 nm, blue line, λ_{ex}= 500 nm red line) and PLE (λ_{em} = 441 nm, blue dashed line). Bottom: PLE (λ_{em} = 561 nm, red dashed line) and phopshorescence (λ_{ex} = 420 nm delay 1 ms, window 10 ms). Bottom:Microscopy images of compound **1** after melting (155°C) and fast cooling the crystalline powders (optical, left and fluorescence, UV excitation, right).

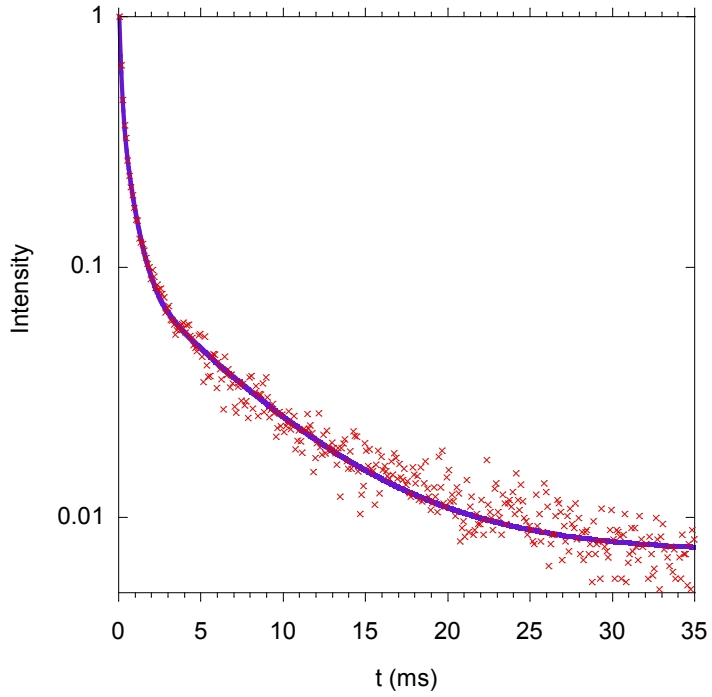

a1	τ_1	a2	τ_2	a3	τ_3	R^2	$\langle\tau\rangle$	τ_{av}
0.08803	6.30484	0.39536	0.65873	0.8107	0.12155	0,99809	0.706281	4,029378

Figure S20. Ph decay of compound **1** as amorphous (red, λ_{ex} = 420 nm, emission 587 nm), and three-exponential fitting (blue line, results are shown in the table).

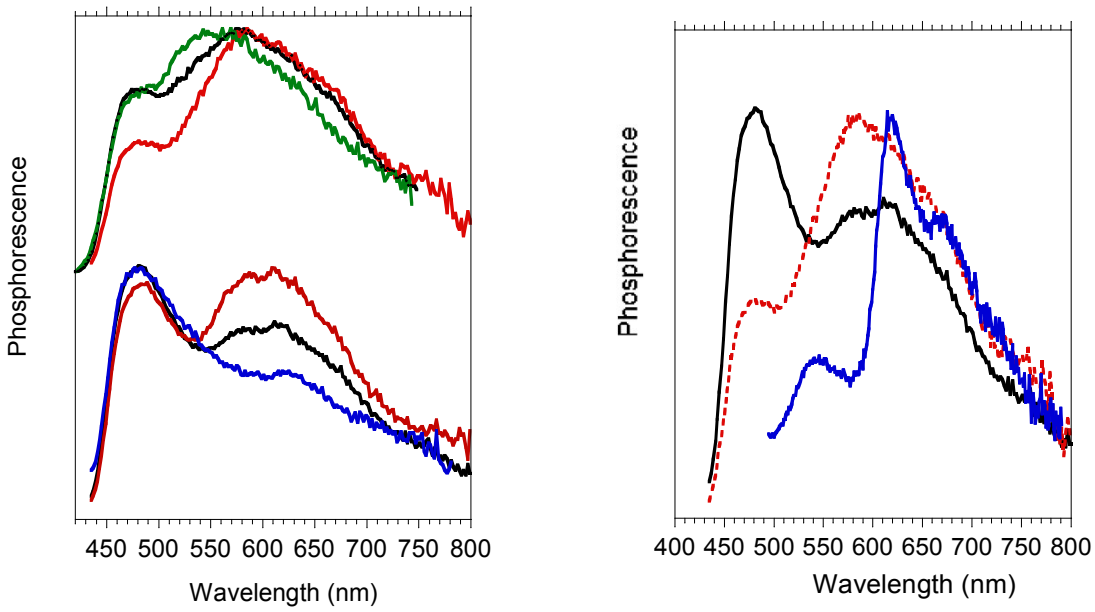

Figure S21. Ph spectra of geminate crystals of compound **3** at different excitations and delay times. ***Left Figure***: Top, excitation 390 nm; delay time 200 ms, window 500 ms, green line; delay 1ms, window 10 ms, black line, delay 5 ms, window 15 ms, red line. Bottom, excitation 420 nm; delay time 200 ms, window 500 ms, blue line; delay 1 ms, window 15 ms, black line, delay 10 ms, window 50 ms, red line. ***Right Figure***: delay time 5 ms, window 15 ms, red line, excitation 390 nm, black line excitation 420 nm, blue line excitation 485 nm.

6. Single Crystal X-ray Diffraction Studies

Table S1. Crystallographic data and structure refinement details for compounds **1** and **2**

	1	**2**
Chemical Formula	$C_{18}H_{16}Br_2N_2O_2$	$C_{18}H_{18}N_2O_2$
Molecular weight	452.15	294.34
T(K)	293(2)	120(2)
Crystal system	Monoclinic	Monoclinic
space group	$P2_1/c$	$P2_1/c$
a(Å)	6.4413(5)	18.21(2)
b(Å)	11.5184(10)	7.066(8)
c(Å)	12.4869(11)	19.77(2)
β(°)	102.8517(13)	110.968(10)
V(Å^3)	903.24(13)	2375(5)
Z	2	6
D_{calcd} (g cm^{-3})	1.662	1.235
μ (mm^{-1})	4.500	0.081
Crystal size (mm)	0.45 x 0.17 x 0.17	0.47 x 0.07 x 0.01
2θmax, °	63.78	50.05
No. of measured, independent and observed [I >2σ(I)] reflections	18004 / 2979 / 2439	25862 / 4084 / 1592
(R_{int})/(R_σ)	0.0200 / 0.0144	0.2842 / 0.1959
data/restraints/params	2979 / 0 / 110	4084 / 0 / 301
R[$F^2 > 2\sigma(F^2)$], wR(F^2)	0.0289, 0.0713	0.0898, 0.2795
S	1.048	0.959
Δρmax, Δρmin (e Å^{-3})	0.567, -0.481	0.476, -0.264

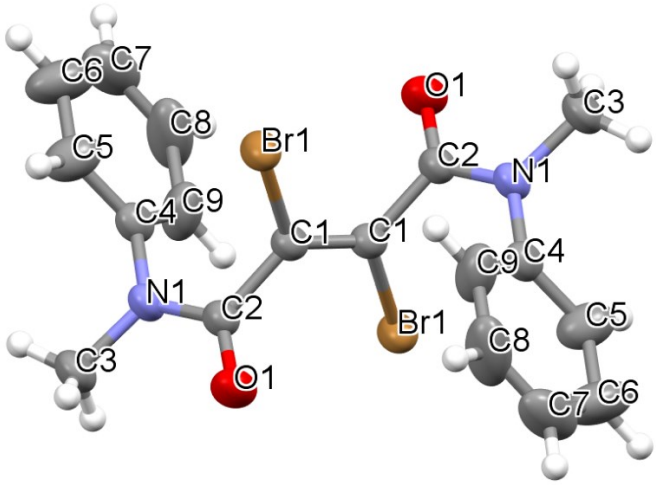

Figure S22. Molecular structure of **1** with atom labelling. Thermal ellipsoids drawn at 50% probability level.

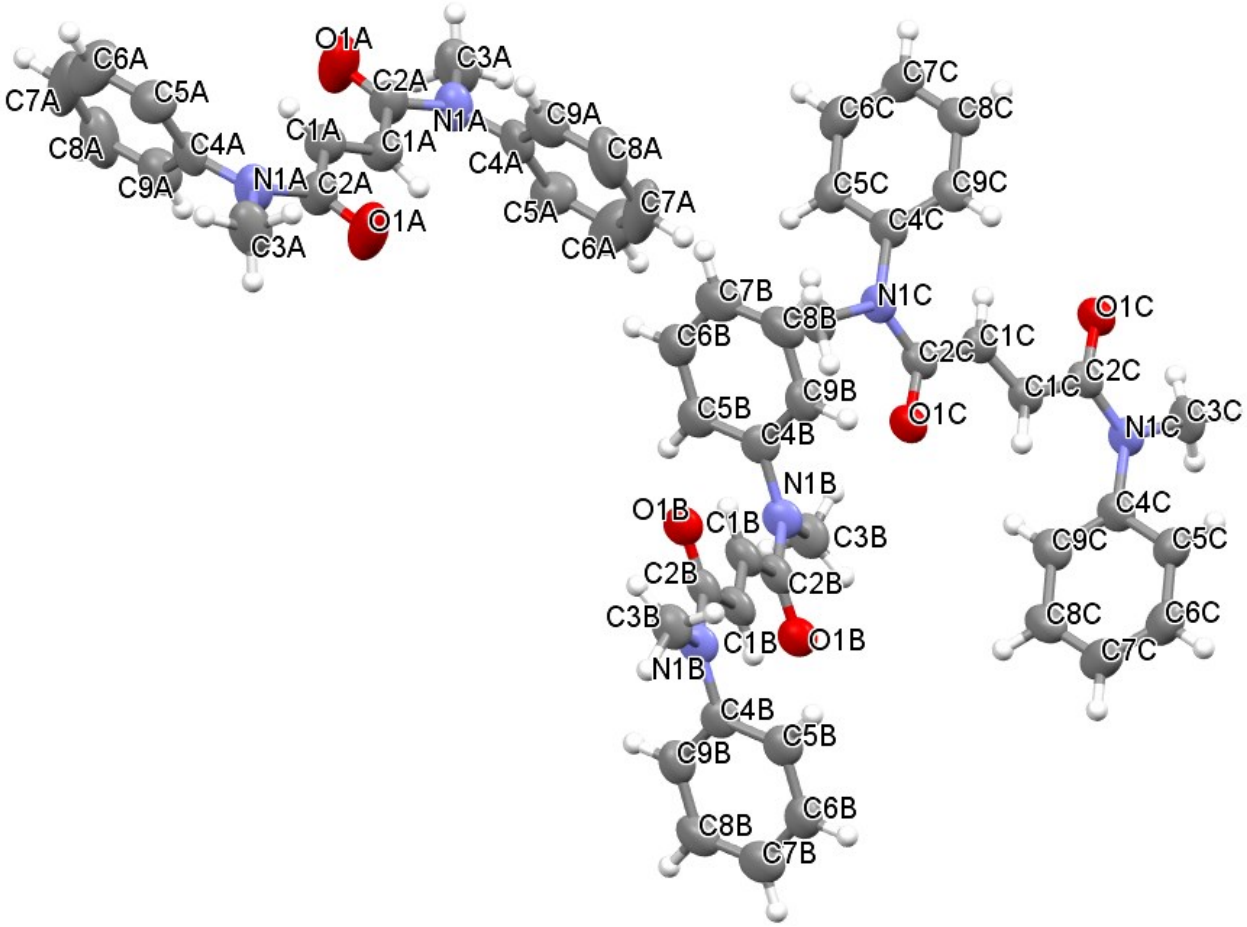

Figure S23. Molecular structure of **2** with atom labelling. Thermal ellipsoids drawn at 50% probability level.

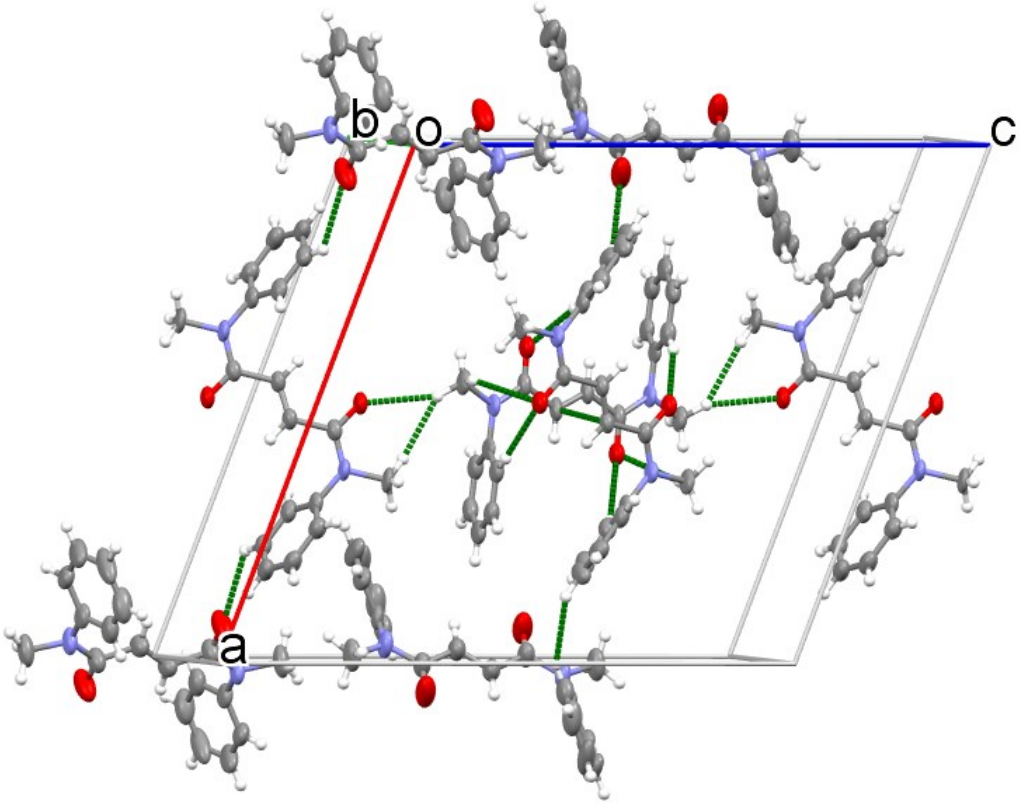

Figure S24. Partial view along b of crystal packing of **2** showing intermolecular contacts (green dashed lines) shorter than the sum of van der Waals radii (ellipsoids at 50 % probability)

7. Characterization of New Compounds

Compound **1**

^{1}H NMR (400 MHz, $CDCl_3$)

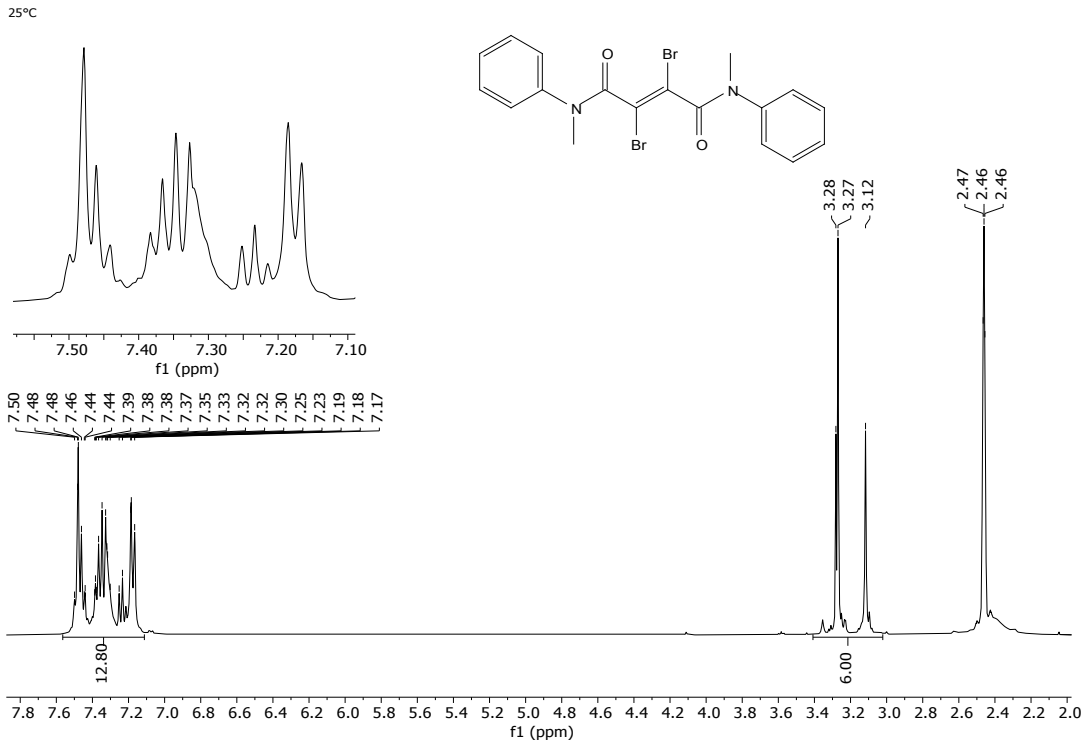

^{13}C NMR (75 MHz, $CDCl_3$)

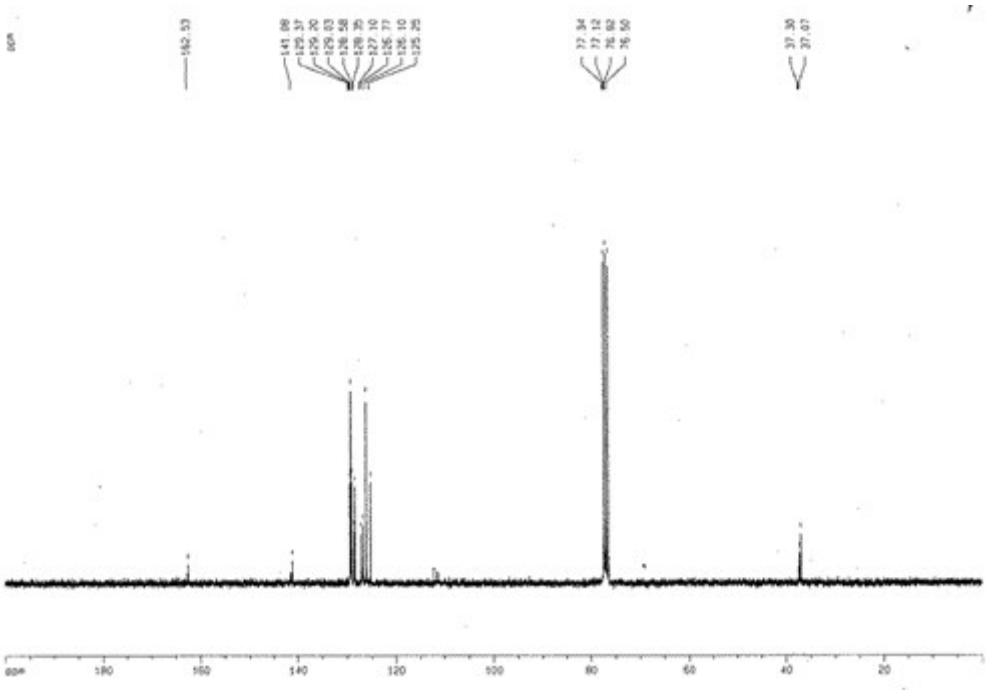

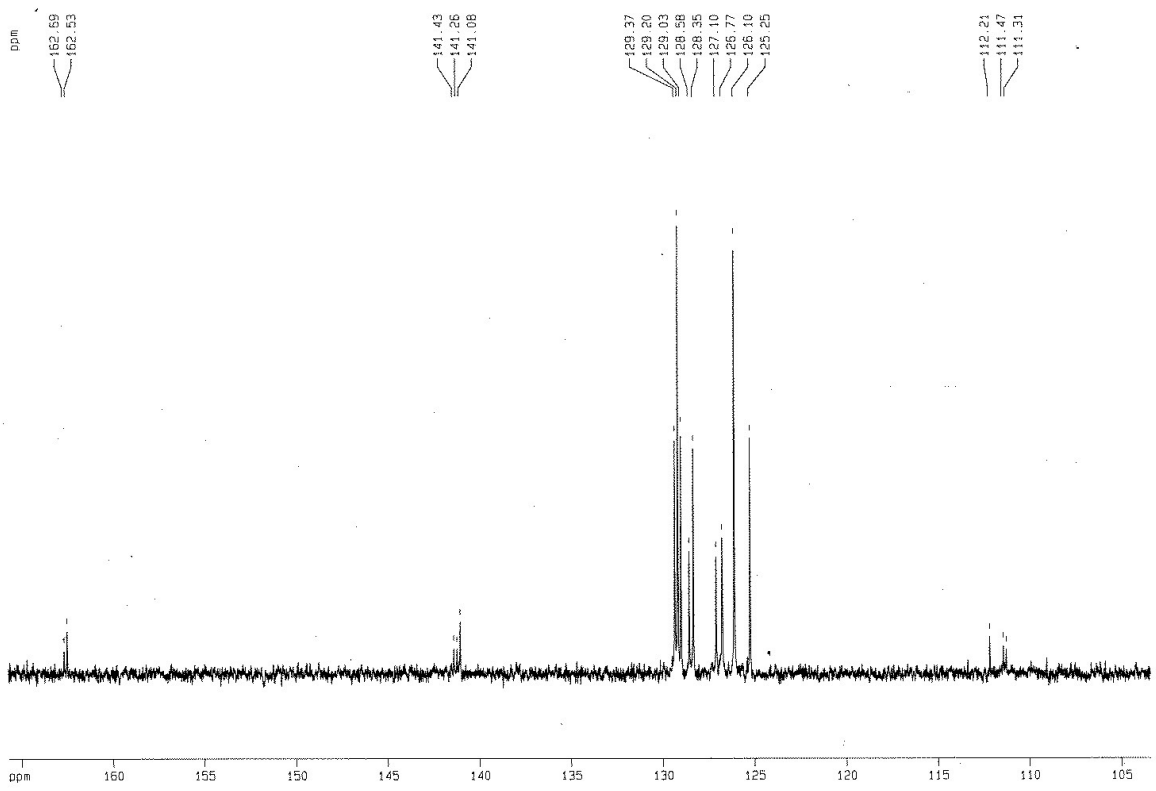
ppm
162.59
162.53
141.43
141.26
141.08
129.37
129.20
129.03
128.58
128.35
127.10
126.77
126.10
125.25
112.21
111.47
111.31
ppm
160
155
150
145
140
135
130
125
120
115
110
105

GC-MS

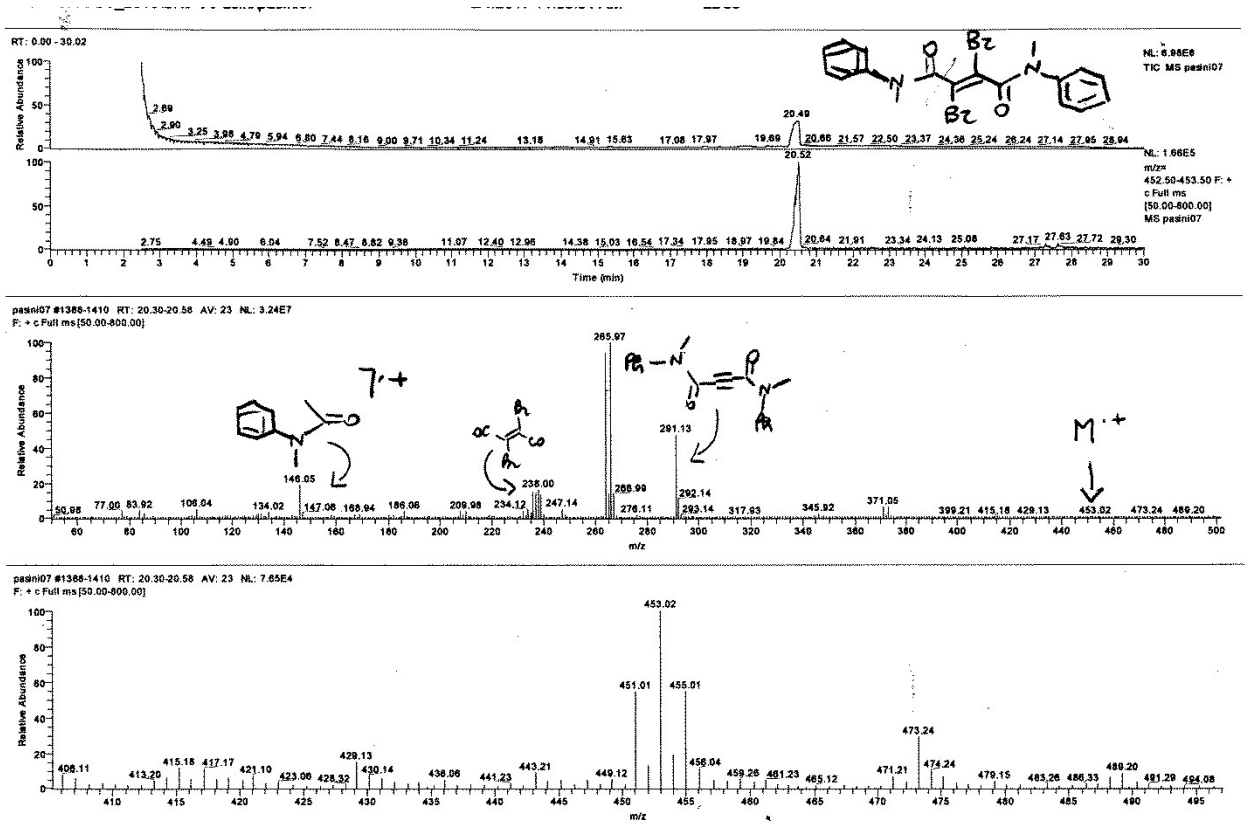
RT: 0.00 - 30.02
Relative Abundance
Time (min)
NL: 6.98E6
TIC MS pasni07
NL: 1.66E5
m/z= 452.50-453.50 F: + c Full ms [50.00-800.00] MS pasni07
pasni07 #1388-1410 RT: 20.30-20.58 AV: 23 NL: 3.24E7
F: + c Full ms [50.00-800.00]
M·+
7·+
m/z
pasni07 #1388-1410 RT: 20.30-20.58 AV: 23 NL: 7.65E4
F: + c Full ms [50.00-800.00]
453.02
451.01
455.01
473.24
m/z

Compound **2**

^{1}H NMR (200 MHz, $CDCl_3$)

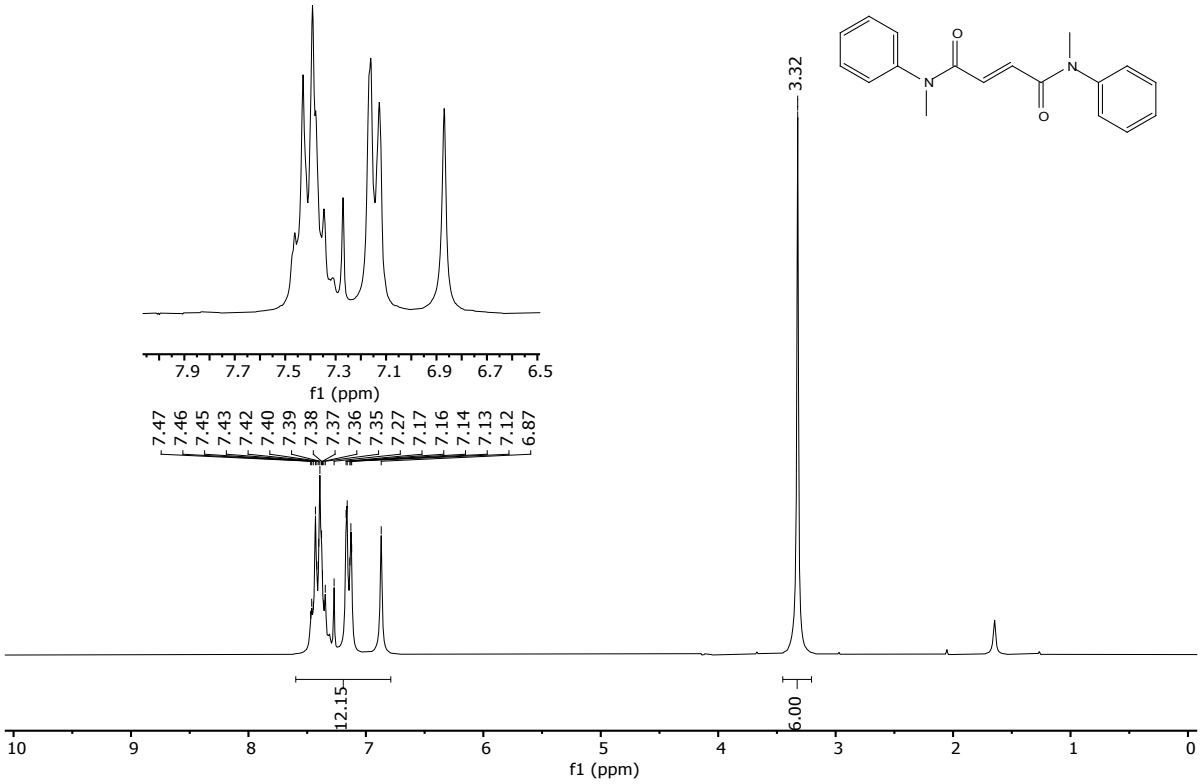

^{13}C NMR (75 MHz, $CDCl_3$) (Asterisk denotes residual MeCN)

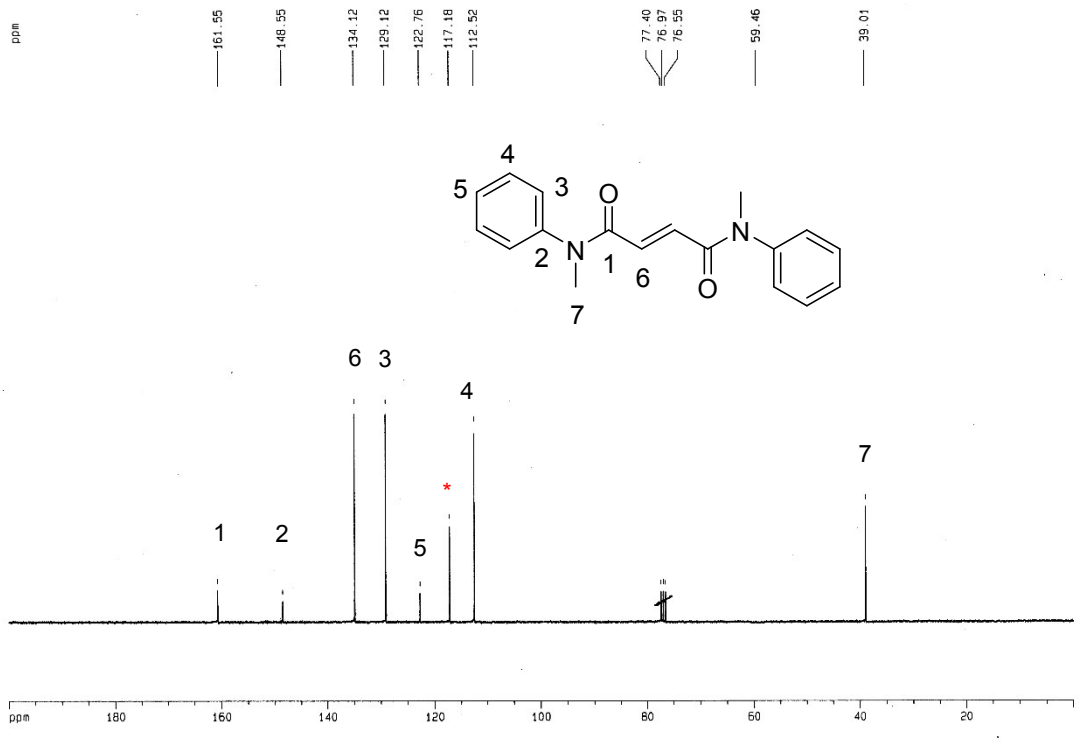

ESI-MS

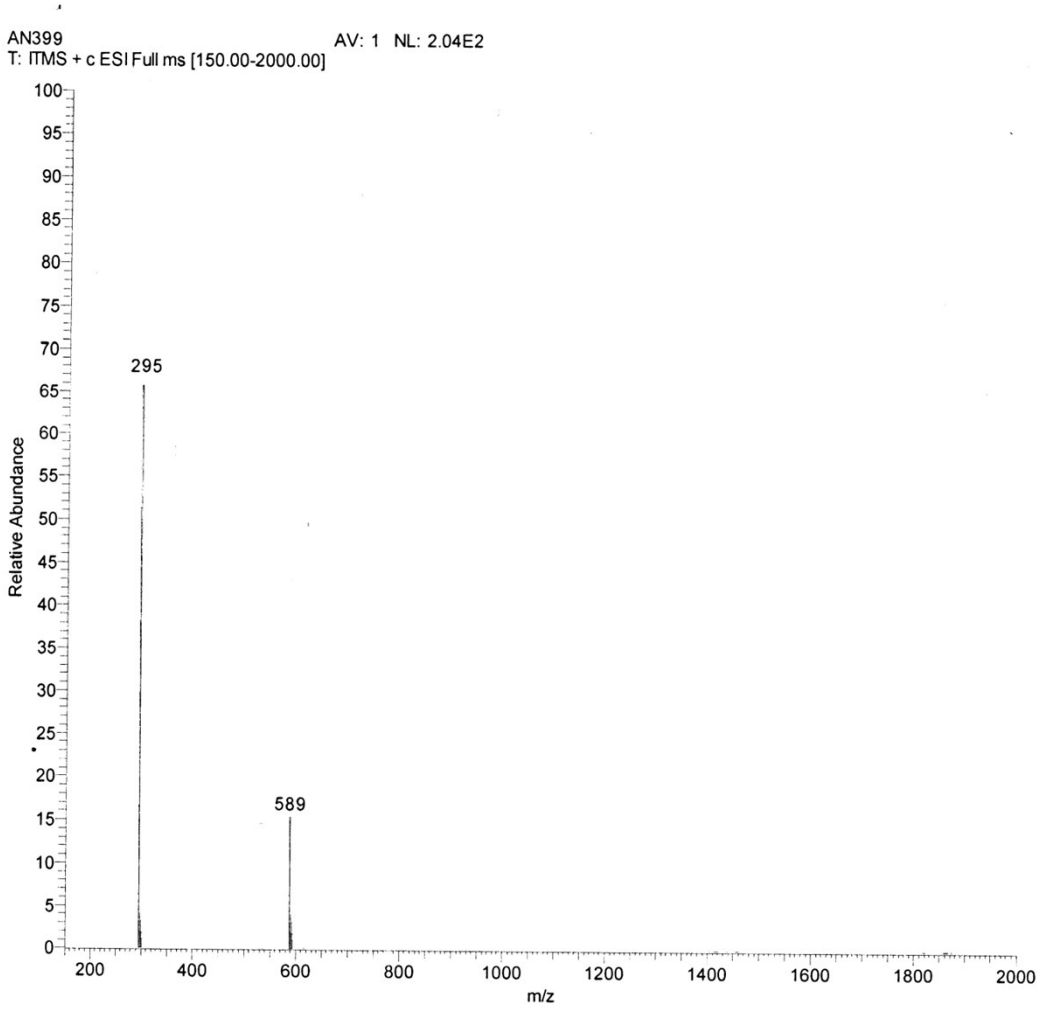
AN399
AV: 1 NL: 2.04E2
T: ITMS + c ESI Full ms [150.00-2000.00]
Relative Abundance
m/z
295
589
100
95
90
85
80
75
70
65
60
55
50
45
40
35
30
25
20
15
10
5
0
200
400
600
800
1000
1200
1400
1600
1800
2000

Compound **3**

^{1}H NMR (300 MHz, $CDCl_3$)

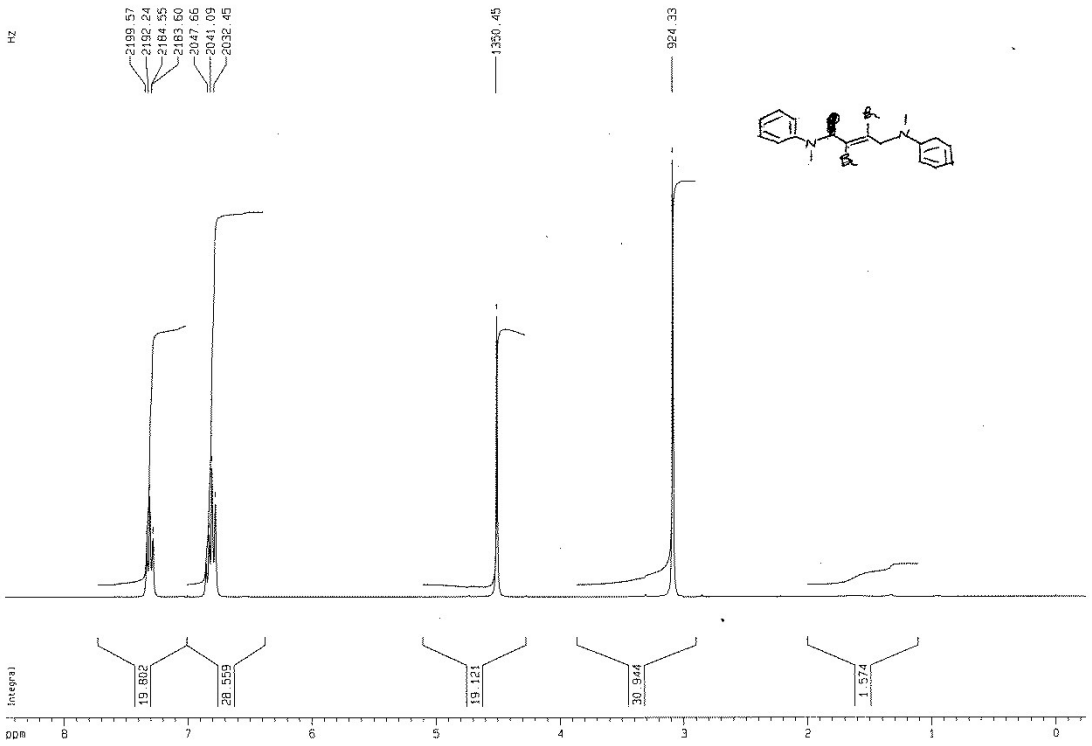

^{13}C NMR (75 MHz, $CDCl_3$)

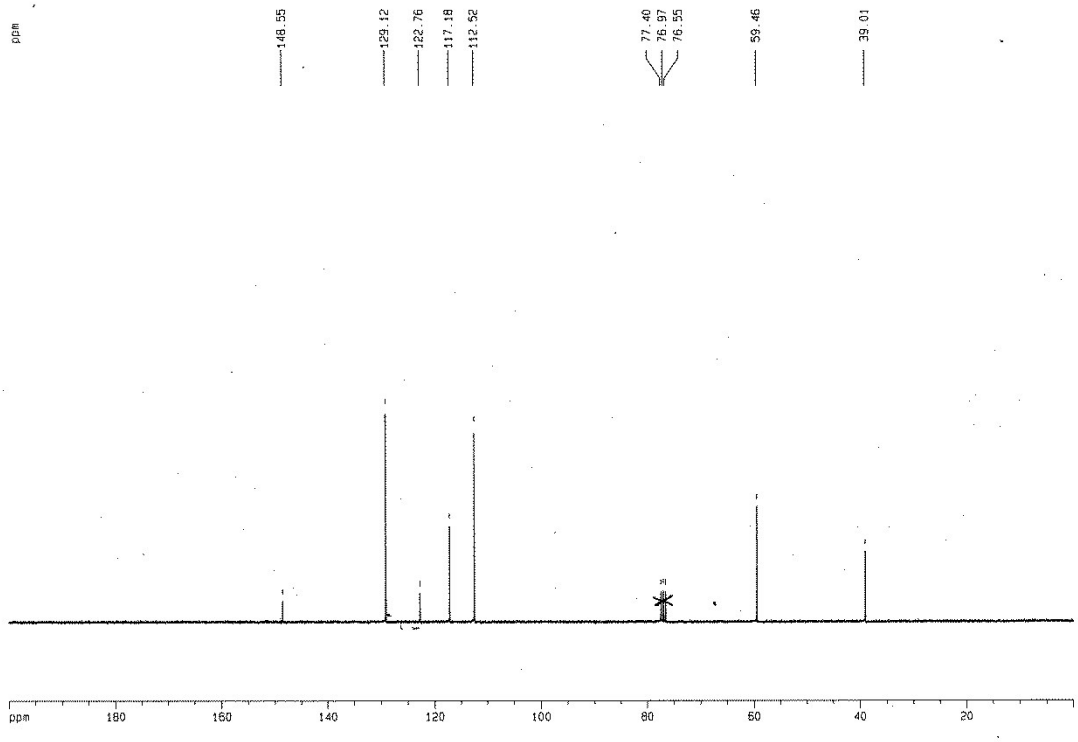

ESI-MS

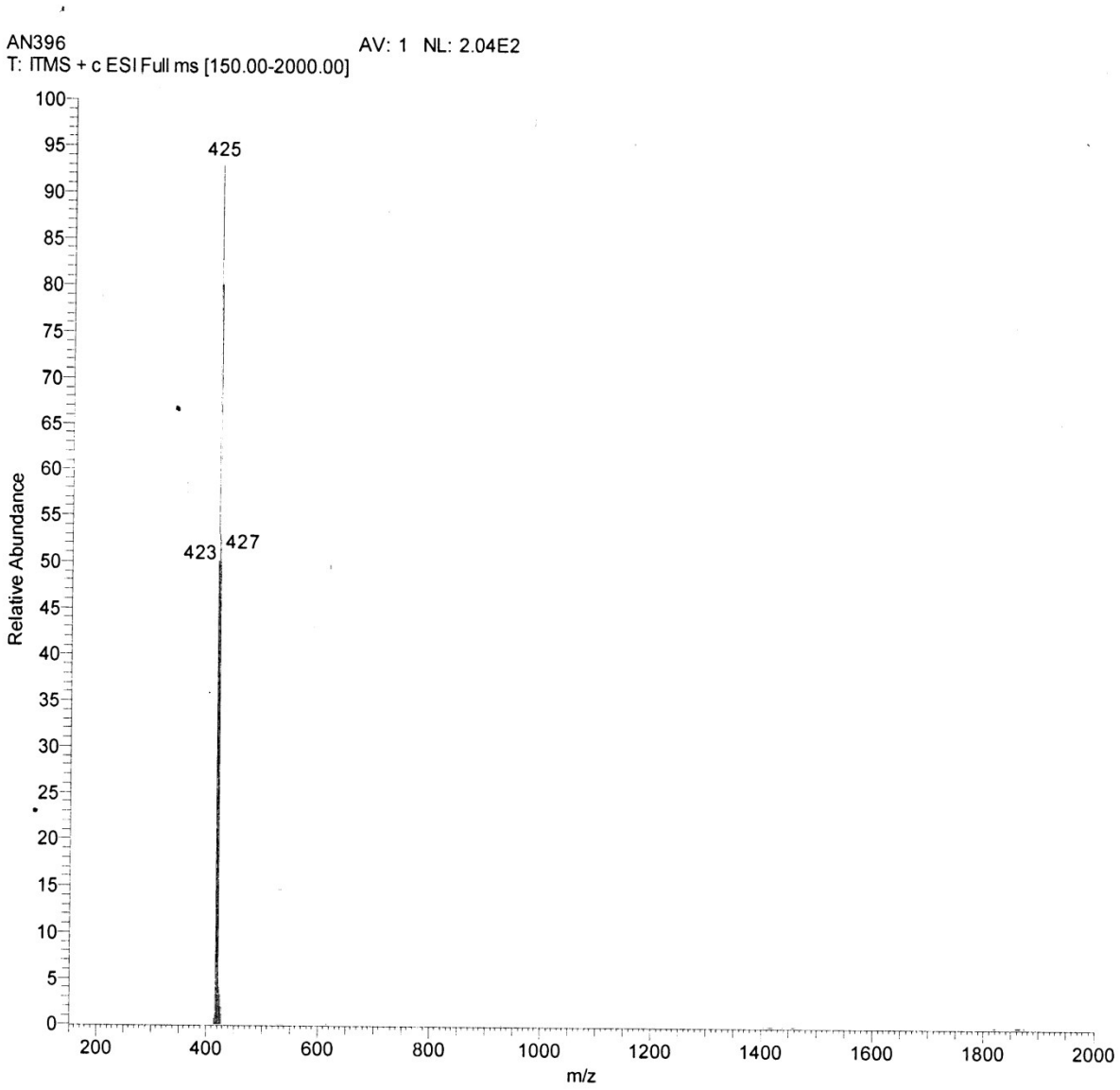
AN396
AV: 1 NL: 2.04E2
T: ITMS + c ESI Full ms [150.00-2000.00]
425
423
427
Relative Abundance
m/z
100
95
90
85
80
75
70
65
60
55
50
45
40
35
30
25
20
15
10
5
0
200
400
600
800
1000
1200
1400
1600
1800
2000

7. Additional References

(S1) J. Moreau at al. *Chem. Phys. Chem.* 2009, **10**, 647-653.

(S2) G. M. Sheldrick, *Acta Crystallogr. C Struct. Chem.* 2015, **71**, 3.

(S3) J.-D. Chai, M. Head-Gordon, *J. Chem. Phys.* 2008, **128**, 084106.

(S4) E. Lucenti, A. Forni, A. Previtali, D. Marinotto, D. Malpicci, S. Righetto, C. Giannini, T. Virgili, P. Kabacinski, L. Ganzer, U. Giovanella, C. Botta, E. Cariati, *Chem. Sci.* 2020, **11**, 7599–7608.

(S5) J. L. Charlton, G. Chee, *Tetrahedron Lett.* 1994, **35**, 6243–6246.

(S6) S. Karabiyikoglu, R. G. Iafe, C. A. Merlic, *Org. Lett.* 2015, **17**, 5248–5251.